THE ASTROPHYSICAL JOURNAL, 601:L51–L54, 2004 January 20

DETECTION OF SAGITTARIUS A* AT 330 MHz WITH THE VERY LARGE ARRAY

MICHAEL E. NORD,[1,2] T. JOSEPH W. LAZIO,[1] NAMIR E. KASSIM,[1] W. M. GOSS,[3] AND N. DURIC[2]
Received 2003 September 30; accepted 2003 December 8; published 2004 January 16

ABSTRACT

We report the detection of Sgr A*, the radio source associated with our Galaxy's central massive black hole, at 330 MHz with the Very Large Array. Implications for the spectrum and emission processes of Sgr A* are discussed and several hypothetical geometries of the central region are considered.

Subject headings: Galaxy: center — Galaxy: nucleus

1. INTRODUCTION

The central radio-bright region of our Galaxy, known as the Sagittarius Complex, is composed of three major components: the supernova remnant (SNR) Sgr A East, the Sgr A West H II region, and Sgr A*, recently established as our Galaxy's central massive black hole (e.g., Ghez et al. 2000; Eckart et al. 2002).

Models attempting to explain the emission from Sgr A* fall into three broad classes. Emission is modeled as arising from thermal sources, such as a low-temperature accretion disk, from nonthermal sources such as a jet (e.g., Melia & Falcke 2001 and references therein), or from a mixture of the two. Such models are constrained primarily by the observed spectrum of Sgr A*, but large gaps in frequency coverage exist. For this reason, filling in such gaps, as with the recent near-IR detections (Ghez et al. 2004; Genzel et al. 2003), and extending the range of frequencies over which the source is observed is important in order to place additional observational constraints on these models.

Davies, Walsh, & Booth (1976) attempted to observe Sgr A* at 410 MHz but reported no detection above a level of 50 mJy. The first Very Large Array[4] (VLA) images of the Galactic center (GC) at 330 MHz (Pedlar et al. 1989; Anantharamaiah et al. 1991) represented a major improvement in sensitivity and resolution over previous meter wavelength images. Pedlar et al. did not detect Sgr A* down to a 5 σ level of 100 mJy. Although Anantharamaiah et al. had higher sensitivity (rms $\sim$3 mJy beam^{-1}), they also reported a nondetection. The absence of any detections below 1000 MHz was interpreted as thermal absorption obscuring Sgr A*, indicating that the low-frequency properties of Sgr A* are dominated by extrinsic absorption, not intrinsic emission.

New low-frequency detections of Sgr A*, including the first detection of the source below 1 GHz (610 MHz; Roy et al. 2003), and this 330 MHz detection suggest that the low-frequency properties of Sgr A* and the implied line of sight optical depths need to be reexamined.

2. OBSERVATIONS AND DATA REDUCTION

The GC was observed at 330 MHz using the VLA in its A configuration; Table 1 summarizes the observations. The visibility amplitudes were calibrated with observations of 3C 286, while the visibility phases were calibrated with observations of the VLA calibrators J1751−253 and J1714−252.

In this Letter we summarize only salient details of the image processing. Full details of the processing including further details on issues such as radio frequency interference excision, astrometry, bandwidth smearing, and extensive details pertaining to calibration and ionospheric compensation will be provided in M. E. Nord et al. (2004, in preparation).

Observations were taken in spectral-line mode to both reduce the impact of bandwidth smearing and enable excision of radio frequency interference. Excision was done manually by searching for visibilities with anomalously high amplitudes, relative to surrounding visibilities in the u-v plane as well as by identifying the Fourier components that gave rise to systematic "ripples" in the image. In general, low-frequency observations with the VLA must take the non-coplanarity of the array into account. Here this was not done because the field of view required to image Sgr A East and West is sufficiently limited ($\approx 3'$) that the array can be assumed to be nearly coplanar. Several iterations of phase-only self-calibration followed by imaging were performed in order to improve the dynamic range of the images and compensate for ionospheric-induced phase distortions. Because data are being combined from different epochs, each epoch was imaged separately to produce an image with an acceptable dynamic range before being combined. The resulting self-calibrated u-v data from the separate epochs were combined and phase and amplitude calibrated against the 1998 image in order to account for any offset in flux density scales and coordinates grids.

In order to obtain maximum resolution, the superuniform weighting scheme (Briggs, Schwab, & Sramek 1999) was used. Superuniform weighting[5] reduces the weight, both globally and locally, given to the central, densely sampled region of the u-v plane, maximizing the resolution at the expense of increased noise and sidelobe level. In this case the increase in noise and sidelobe level is an acceptable trade-off, as the analysis is limited more by the u-v coverage and resulting image fidelity than by the thermal noise level. Figure 1 shows the superuniform image of the Sgr A* region.

3. ANALYSIS

3.1. *Predicted Characteristics of Sgr A* at* 330 MHz

The expected size of Sgr A* was calculated from the measurements from 5 to 45 GHz by R. G. Bower et al. (2004, in preparation). They find the scattering disk of Sgr A* to be $(1.39 \pm 0.02) \times 0.65^{+0.11}_{-0.14}$ mas at $\lambda = 1$ cm. Scaling these di-

[1] Naval Research Laboratory, Code 7213, 4555 Overlook Avenue, Washington, DC 20375-5351; michael.nord@nrl.navy.mil, joseph.lazio@nrl.navy.mil, namir.kassim@nrl.navy.mil.

[2] Department of Physics and Astronomy, University of New Mexico, 800 Yale Boulevard NE, Albuquerque, NM 87131; duric@tesla.phys.unm.edu.

[3] National Radio Astronomy Observatory, P.O. Box O, Socorro, NM 87801; mgoss@nrao.edu.

[4] The VLA is operated by the National Radio Astronomy Observatory, which is a facility of the National Science Foundation, operated under cooperative agreement by Associated Universities, Inc.

[5] UVBOX = 3 and ROBUST = −1 within the AIPS task IMAGR.

TABLE 1
OBSERVATIONAL SUMMARY

Epoch	Configuration	ν (MHz)	$\Delta\nu$ (MHz)	Integration (hr)
1996 Oct	A	332.5	6	5.6
1998 Mar	A	327.5	3	5.4

mensions by λ^2 as expected from interstellar scattering gives an expected 330 MHz diameter of $(11.5 \pm 0.2) \times 5.4^{+0.9}_{-1.1}$ arcsec. The position angle of the scattering disk of Sgr A* is constant at ~80° over the range of 1.4–46 GHz. We have assumed that its orientation remains constant below 1.4 GHz. Sgr A* has a time-averaged flux density at 1.4 GHz of ≈0.5 Jy and a time-averaged spectral index over the centimeter radio regime of $\alpha \sim 0.3$ ($S_\nu \propto \nu^\alpha$) (Zhao, Bower, & Goss 2001). Assuming no change in the spectral index below 1.4 GHz, the expected 330 MHz flux density is roughly 0.4 Jy.

3.2. *The Detection of Sgr A**

Figure 2 shows slices through the assumed major and minor axes of Sgr A*. Gaussian fits with baseline subtraction to these slices results in a measured source size of $(17\farcs6 \pm 4'') \times (15\farcs9 \pm 5'')$, a peak intensity of 80 ± 15 mJy beam^{-1}, and a total flux density of 330 ± 120 mJy. The source deconvolved with the $6\farcs8 \times 10\farcs9$ beam gives a source size of $(16'' \pm 4'') \times (11'' \pm 5'')$. If the source is fit in the image instead of fitting slices, the position angle is then a free parameter instead of assumed to be 80°. A two-dimensional Gaussian fit of the region yields a position angle of 35° ± 35°. However, this fit is contaminated by flux density to the south of the source as shown in the slice on the right in Figure 2.

The location and flux density of the source agree with the extrapolations of § 3.1, and the size of the source agrees to within ~1.2 σ along the assumed minor axis and ~1.1 σ along the assumed major axis. However, an alternate interpretation of this emission is that it originates from the Sgr A East SNR.

The absorption in Figure 1 is caused by the Sgr A West H II region, first detected in absorption by Pedlar et al. (1989). The Sgr A West H II region is composed of a dense region known as the "minispiral" (Lo & Claussen 1983; Ekers et al. 1983), known to be orbiting Sgr A* (Roberts and Goss 1993), and a more diffuse ionized region ≈80″ × 60″ in size, known as Sgr A West (extended; Mezger & Wink 1986; Pedlar et al. 1989). Both components of Sgr A West are detected in thermal (free-free) absorp-

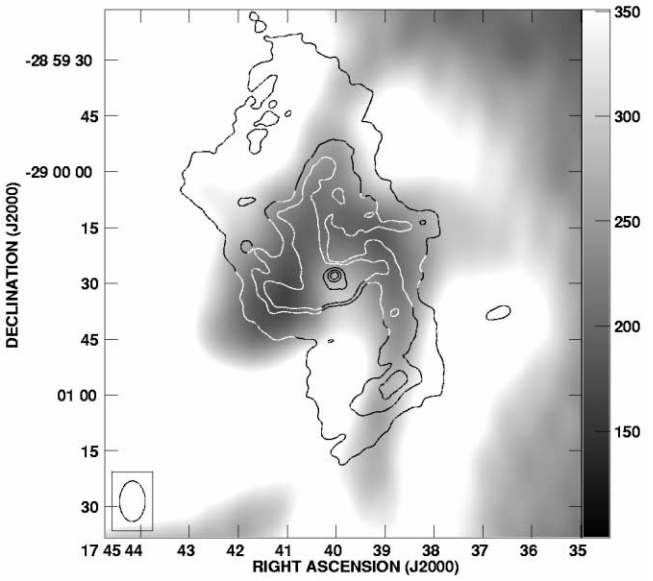

FIG. 1.—Superuniform image of the Sgr A* region at 330 MHz. White areas represent areas of high brightness; dark areas represent areas of lower brightness due to absorption of the Sgr A East SNR by Sgr A West minispiral and Sgr A West (extended). The gray scale is linear between 100 and 350 mJy beam^{-1}. The resolution is $6\farcs8 \times 10\farcs9$ with a position angle of −1° and an rms noise of ~4 mJy beam^{-1}. Contours are 5 GHz (Yusef-Zadeh & Morris 1987) with a resolution of $3\farcs4 \times 2\farcs9$, position angle of −80°, and levels of 1, 2, 3, 9, 15, 20, 25, and 30 times 40 mJy beam^{-1}. Sgr A* is located at the position of maximum 5 GHz intensity. Note the 330 MHz absorption and the 5 GHz diffuse flux density correlate well except at the position of Sgr A*, where the 5 GHz is maximum and the 330 MHz is at a local maximum.

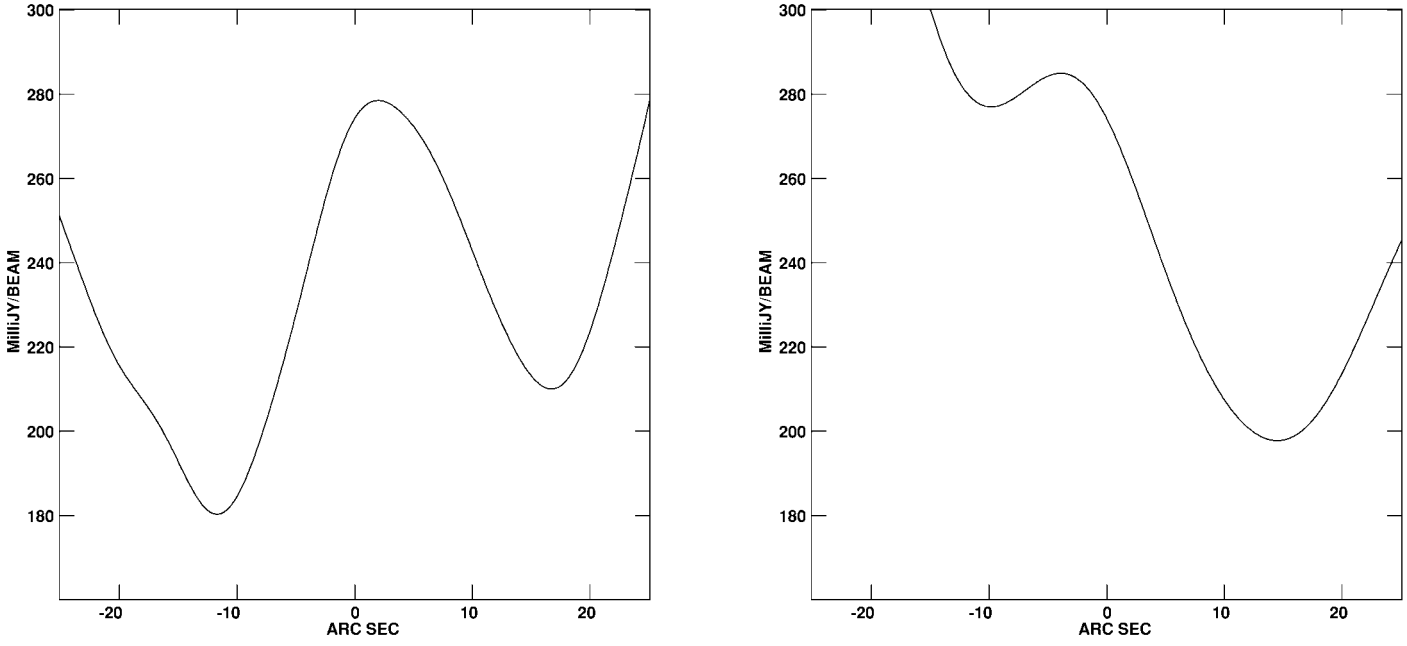

FIG. 2.—*Left*: Slice through the expected major axis of Sgr A* in Fig. 1. The slice is centered at $17^h45^m40^s$, −29°00′28″ with a position angle of 80° (J2000.0) and a resolution of ~6″.8. East is toward the left. *Right*: Slice through the expected minor axis of Sgr A* in Fig. 1. Resolution is ~10″.9. South is toward the left.

tion against the Sgr A East SNR with 330 MHz optical depths (τ_{330}) greater than 1 across a large portion of the H II region (Pedlar et al. 1989). The position of Sgr A* is offset from the minispiral (Zhao & Goss 1998); therefore, in order for Sgr A East to be absorbed at the position of Sgr A*, most of the absorption must arise from Sgr A West (extended). Estimates of the optical depth along lines of sight near Sgr A* based on higher frequency measurements ($\nu = 5$ GHz; Yusef-Zadeh & Morris 1987) suggest that 330 MHz optical depths near Sgr A* are $\tau_{330} \sim 10$. Moreover, any gap through the Sgr A West H II region would have to occur with the size, shape, and location necessary to allow Sgr A East to be detected with the expected size, shape, and flux density of Sgr A*. Given the agreement in observed and predicted source properties, the likelihood that Sgr A East is detected can be discounted. We conclude that we have detected Sgr A* at 330 MHz.

4. IMPLICATIONS

4.1. *Previous Nondetections*

Previous nondetections at similar frequencies can be attributed to the limited sensitivities of the observations. Davies et al. (1976) observed using the Mk I–Defford interferometer. This two-element interferometer has a north-south resolution of $\theta \approx 2\farcs4$ at 408 MHz. The correlated flux density that would have been measured by this interferometer is $S_{\rm corr} = S_0 e^{-(\theta_s/\theta)^2}$, where θ_s is the scattering diameter and S_0 is the intrinsic flux density (Roy et al. 2003). The expected scattering diameter of Sgr A* is $4\farcs1$. Their upper limit, $S_{\rm corr} < 50$ mJy, implies that they would not have detected any source weaker than 0.9 Jy, a value that is well above the flux density that we have observed at 330 MHz.

Pedlar et al. (1989) observed the GC with the VLA. At the time of their observations, only a few (~10) of the 27 VLA antennas were outfitted for 330 MHz observations. In addition to a higher thermal noise level (rms sensitivity ≈16 mJy beam^{-1}), the number of baselines was substantially lower, resulting in less complete u-v coverage. Sgr A* would have been only a 3 σ source in a crowded and confusing field.

Anantharamaiah, Pedlar, & Goss (1999) reanalyzed data from Anantharamaiah et al. (1991) in which the GC was observed at 330 MHz with all antennas of the VLA. In their Figure 2, there is a hint of a detection of Sgr A* at a level of ~40 mJy beam^{-1}, which is consistent with this detection. The authors do not comment on this possible detection.

4.2. *The Spectrum of Sgr A**

Figure 3 shows the observed spectrum for Sgr A*, including our flux density measurement. This spectrum is not constructed from simultaneous measurements, and because Sgr A* is variable, simultaneous measurements may show differences.

There are at least two models of the low-frequency spectrum of Sgr A* that are suggested by our detection. Either the $S_\nu \propto \nu^{0.3}$ spectrum observed across the centimeter radio band continues toward low frequencies and the source is unobscured by intervening thermal gas, or the spectrum of Sgr A* rises below ~1 GHz and is obscured by significant optical depth.

Assuming a $S_\nu \propto \nu^{0.3}$ spectrum, a 330 MHz optical depth of $\tau_{330} < 0.1$ is required to explain the measured Sgr A* flux density. Even a flat spectrum below 1.4 GHz permits an optical depth of only $\tau_{330} \sim 0.4$. Therefore, the free-free optical depth along this line of sight is much less than the $\tau_{330} \sim 3$–5 previously assumed to explain low-frequency nondetections (Pedlar et al. 1989).

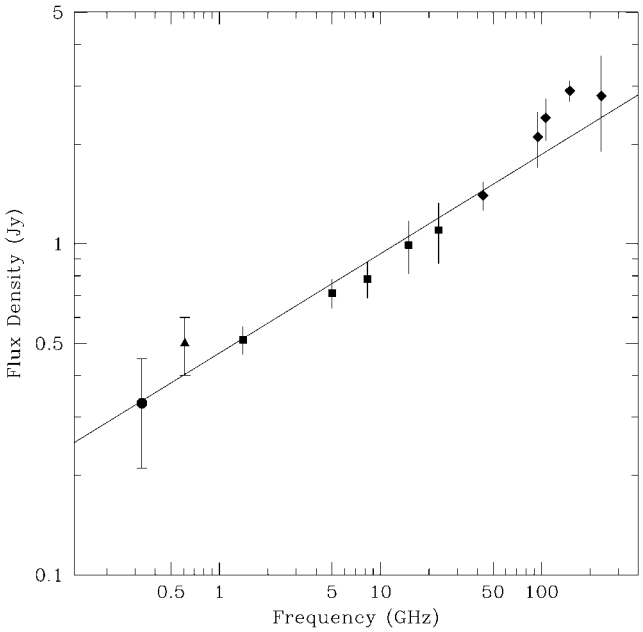

FIG. 3.—Radio/submillimeter ($0.33 < \nu < 235$ GHz) spectrum of Sgr A*. Bars without endcaps signify variability limits. The 610 MHz value is from Roy et al. (2003). The $1.4 < \nu < 23$ GHz values (*squares*) are from Zhao et al. (2001). These data are time-averaged over 1980–2000. The $43 < \nu < 235$ GHz values (*diamonds*) are from Falcke et al. (1998) and are averaged over 1987–1994. For reference, the solid line indicates a spectrum with spectral index 0.3; it is not a fit to the data. The low-frequency spectral index is $\alpha_{330}^{1400} = 0.3^{+0.5}_{-0.4}$.

A conclusion of § 3.2 is that lines of sight to Sgr A East that pass near Sgr A* have large 330 MHz optical depths. If the line of sight to Sgr A* were similarly obscured, its intrinsic flux density would have to be increasing at low frequencies in order to agree with the observed flux density. The optical depth has a frequency dependence of $\nu^{-2.1}$. In order to agree with the observed flux density, the intrinsic flux density would have to rise exponentially ($S_\nu \propto e^{\nu^{-2.1}}$) below ~1 GHz.

Low 330 MHz optical depths near Sgr A* are also indicated by the 22 GHz, $0\farcs1$ resolution image of the Sgr A* region by Zhao & Goss (1998), which shows emission measures due to ionized gas within $0\farcs2$ of Sgr A* are nearly 2 orders of magnitude lower than in the nearby minispiral. Furthermore, an exponential rise in intrinsic flux density to almost exactly cancel the large (factor of ~10 between 1000 and 330 MHz) increase in free-free optical depth at 330 MHz would be quite improbable.

We conclude that it is likely that there is little or no free-free absorption along the line of sight to Sgr A*, and that the observed flux density is intrinsic to the source. Our results imply a large optical depth toward the Sgr A East SNR, but a small optical depth toward Sgr A*. This could be explained by a localized clearing of the ambient gas accomplished either through the direct influence of the black hole, or through the stellar winds of the central cluster. It is also possible that the ionized medium in the GC region is clumped, with the line of sight to Sgr A* passing through a gap. Our data cannot differentiate between these possibilities.

4.3. *Emission Mechanisms*

Previous modeling of the spectrum of Sgr A* did not have to confront its flux density at low frequencies, because Sgr A* was thought to be unobservable below 1 GHz (e.g., Mahadevan 1998). Furthermore, the 410 MHz nondetection of Davies et

al. (1976) is often incorrectly treated as an upper limit. Our 330 MHz result and the 610 MHz detection by Roy et al. (2003) require these models to be reevaluated. Because we cannot exclude the possibility of free-free optical depth toward Sgr A*, our reported 330 MHz flux density should be considered a *lower* limit.

Advection-dominated accretion flow (ADAF) models (e.g., Yuan, Markoff, & Falcke 2002) predict flux densities nearly 2 orders of magnitude lower than the 330 MHz measurement. The relativistic jet+ADAF model of Yuan et al. (2002) does not explicitly make predictions below 1.4 GHz but would appear to closely match the measured 330 MHz flux density. It should be noted that in the jet models, low-frequency emission arises from farther out along the jet, probing regions farther from the event horizon.

5. CONCLUSIONS

We have presented a new high-resolution, high-sensitivity image of the Sgr A region at 330 MHz, constructed from observations at multiple epochs with the Very Large Array. We report a detection of Sgr A*, with a flux density of 330 ± 120 mJy. Previous nondetections of Sgr A* at comparable frequencies are attributable to the poor sensitivity and/or *u*-*v* coverage of the interferometers used.

We argue that only small amounts of free-free absorption ($\tau_{330} \sim 0.1$) exist along the line of sight to Sgr A* and therefore that Sgr A* is observed through a region of low density in the Sgr A West H II region. It is possible that the intrinsic spectrum of Sgr A* rises below ~1 GHz. However, the intrinsic rise in flux density would have to be balanced by free-free absorption to result in the observed value. Therefore, this flux density measurement is a *lower* limit to the intrinsic flux density of this source as the optical depth along the line of sight remains unknown (e.g., Anantharamaiah et al. 1999).

This detection at 330 MHz, combined with the recent detection at 610 MHz (Roy et al. 2003), expands the frequency range over which Sgr A* has been detected and allows for low-frequency observational constraints on Sgr A* emission mechanisms. Future observations at and below 240 MHz with the Giant Metrewave Radio Telescope and the Low Frequency Array (Kassim et al. 2000) may expand the frequency range at which Sgr A* is detectable to even lower frequencies.

We thank G. Bower for the use of unpublished results pertaining to the scattering size of Sgr A*, C. Brogan for help with data reduction and imaging, and A. Cohen and L. J. Rickard for helpful discussions. Basic research in radio astronomy at the NRL is supported by the Office of Naval Research. The National Radio Astronomy Observatory is a facility of the National Science Foundation operated under cooperative agreement by Associated Universities, Inc.

REFERENCES

Anantharamaiah, K. R., Pedlar, A., Ekers, R. D., & Goss, W. M. 1991, MNRAS, 249, 262
Anantharamaiah, K. R., Pedlar, A., & Goss, W. M. 1999, in ASP Conf. Ser. 186, The Central Parsecs of the Galaxy, ed. H. Falcke, A. Cotera, W. J. Duschl, F. Melia, & M. J. Rieke (San Francisco: ASP), 422
Briggs, D. S., Schwab, F. R., & Sramek, R. A. 1999, in ASP Conf. Ser. 180, Synthesis Imaging in Radio Astronomy II, ed. G. B. Taylor, C. L. Carilli, & R. A. Perley (San Francisco: ASP), 127
Davies, R. D., Walsh, D., & Booth, R. S. 1976, MNRAS, 177, 319
Eckart, A., Genzel, R., Ott, T., & Schödel, R. 2002, MNRAS, 331, 917
Ekers, R. D., van Gorkom, J. H., Schwarz, U. J., & Goss, W. M. 1983, A&A, 122, 143
Falcke, H., Goss, W. M., Matsuo, H., Teuben, P., Zhao, J., & Zylka, R. 1998, ApJ, 499, 731
Genzel, R., Schödel, T., Ott, T., Eckart, A., Alexander, T., Lacombe, F., Rouan, D., & Aschenbach, B. 2003, Nature, 425, 934
Ghez, A. M., Morris, M., Becklin, E. E., Tanner, A., & Kremenek, T. 2000, Nature, 407, 349
Ghez, A. M., et al. 2004, ApJ, in press
Kassim, N. E., Lazio, T. J. W., Erickson, W. C., Crane, P. C., Perley, R. A., & Hicks, B. 2000, Proc. SPIE, 4015, 328
Lo, K. Y., & Claussen, M. J. 1983, Nature, 306, 647
Mahadevan, R. 1998, Nature, 394, 651
Melia, F., & Falcke, H. 2001, ARA&A, 39, 309
Mezger, P. G., & Wink, J. E. 1986, A&A, 157, 252
Pedlar, A., Anantharamaiah, K. R., Ekers, R. D., Goss, W. M., van Gorkom, J. H., Schwarz, U. J., & Zhao, J. 1989, ApJ, 342, 769
Roberts, D. A., & Goss, W. M. 1993, ApJS, 86, 133
Roy, S., et al. 2003, Astron. Nachr., 324, S1
Yuan, F., Markoff, S., & Falcke, H. 2002, A&A, 383, 854
Yusef-Zadeh, F., & Morris, M. 1987, ApJ, 322, 721
Zhao, J., Bower, G. C., & Goss, W. M. 2001, ApJ, 547, L29
Zhao, J., & Goss, W. M. 1998, ApJ, 499, L163